Editors' Suggestion | Featured in Physics

Magnetic Lyddane-Sachs-Teller Relation

Viktor Rindert,[1,*] Vanya Darakchieva,[1,2] Tapati Sarkar,[3] and Mathias Schubert[4,1]
[1]NanoLund and Solid State Physics, Lund University, S-22100 Lund, Sweden
[2]Department of Physics, Chemistry, and Biology (IFM), Linköping University, SE 58183 Linköping, Sweden
[3]Department of Materials Science and Engineering, Uppsala University, Box 35, SE-751 03 Uppsala, Sweden
[4]Department of Electrical and Computer Engineering, University of Nebraska-Lincoln, Lincoln, Nebraska 68588, USA

(Received 27 May 2024; revised 19 December 2024; accepted 24 December 2024; published 26 February 2025)

We describe a magnetic relation in analogy to the well-known dielectric Lyddane-Sachs-Teller relation [R. H. Lyddane *et al.*, Phys. Rev. **59**, 673 (1941)]. This magnetic relation follows directly from the model equations for nuclear induction due to fast oscillating electromagnetic fields [F. Bloch, Phys. Rev. **70**, 460 (1946)] and relates the static permeability with the product over all ratios of antiresonance and resonance frequencies associated with all magnetic excitations within a given specimen. The magnetic relation differs significantly from its dielectric analog where the static properties are related to ratios of the squares of resonance frequencies. We demonstrate the validity of the magnetic Lyddane-Sachs-Teller relation using optical magnetization data from terahertz electron magnetic resonance spectroscopic ellipsometry measurements in the presence of an external magnetic field on an iron-doped semiconductor crystal of gallium nitride.

DOI: 10.1103/PhysRevLett.134.086703

Introduction—We describe here a fundamental law in magnetism that relates static properties with optical phenomena in magnetism. This law—which we will term here the magnetic Lyddane-Sachs-Teller relation—has a well-known analog—the dielectric Lyddane-Sachs-Teller (LST) relation [1]. The latter was described by Teller *et al.* within a seminal paper in 1941. This fundamental law has since entered textbooks in solid-state physics [2]. We derive the magnetic relation here from another, equally important contribution in physics, the nuclear induction paper by Bloch on the interaction of nuclear magnetic moments with fast oscillating electromagnetic fields [3]. This 1946 paper led to the discovery of magnetic resonance, which today is perhaps one of the most widespread techniques used in science. The magnetic relation derived here is similar, yet differs significantly from its dielectric analog as will be discussed further below. We demonstrate here the validity of the magnetic Lyddane-Sachs-Teller relation using optical magnetization data available from terahertz spectroscopic ellipsometry measurements on an iron-doped semiconductor crystal of gallium nitride. We developed instruments recently to measure magnetic resonance as predicted by Bloch continuously as a function of frequency and with complete polarization information [4]. Analysis of poles and zeros of the real and imaginary parts of the permeability function provides access to magnetic resonance and antiresonance frequencies analogous to the transverse and longitudinal optical frequencies in the dielectric function across dielectric lattice mode excitations. Thus, we can also demonstrate here experimental evidence for the correctness of the magnetic Lyddane-Sachs-Teller relation.

The LST relation establishes a fundamental equality between two critical ratios in materials exhibiting optical lattice vibrations [1]. Specifically, the relation equates the square of the ratio of frequencies between longitudinal optic (LO; ω_{LO}) and transverse optic (TO; ω_{TO}) lattice vibrations at long wavelengths, for ionic crystals with one optical phonon branch, with the ratio of the static ($\varepsilon_{\mathrm{dc}}$) and high-frequency dielectric permeability (ε_{∞}),

$$\frac{\varepsilon_{\mathrm{dc}}}{\varepsilon_{\infty}} = \frac{\omega_{\mathrm{LO}}^2}{\omega_{\mathrm{TO}}^2}. \tag{1}$$

Transverse resonance occurs at very large displacement and longitudinal resonance occurs when the field-induced polarization compensates its vacuum contribution (antiresonance). For materials with multiple (N) optical phonon branches, extensions to the LST relation have been made by Barker [5] and Berreman and Unterwald [6],

$$\frac{\epsilon_{\mathrm{dc}}}{\epsilon_{\infty}} = \prod_{l=1}^{N} \frac{\omega_{\mathrm{LO,l}}^2}{\omega_{\mathrm{TO,l}}^2}. \tag{2}$$

Further generalizations have been proposed by Cochran and Cowley [7], who have extended the theory to include

*Contact author: viktor.rindert@ftf.lth.se

Published by the American Physical Society under the terms of the Creative Commons Attribution 4.0 International license. Further distribution of this work must maintain attribution to the author(s) and the published article's title, journal citation, and DOI. Funded by Bibsam.

the phonon displacement vector. This version is applicable when the principal polarization axes align with orthogonal directions. A coordinate invariant LST relation was introduced, which holds for all crystal symmetries, including monoclinic and triclinic [8]. The coordinate invariant LST relation was derived from the microscopic Born-Huang description of polar lattice vibrations and relates the determinant of the permittivity tensor at zero and infinite frequencies to the LO and TO resonance modes defined thereby [8],

$$\det[\boldsymbol{\epsilon}^{-1}(\omega_{\mathrm{TO}})] = 0, \qquad \det[\boldsymbol{\epsilon}(\omega_{\mathrm{LO}})] = 0, \tag{3}$$

$$\frac{\det[\boldsymbol{\epsilon}(\omega = 0)]}{\det(\boldsymbol{\epsilon}_{\infty})} = \prod_{l=1}^{N} \frac{\omega_{\mathrm{LO},l}^2}{\omega_{\mathrm{TO},l}^2}. \tag{4}$$

This generalization has proved pivotal in analyzing phonon modes in monoclinic crystal structures, advancing our understanding of material properties [9–13].

In this Letter, we extend the concept of the LST relation toward magnetic dipole transitions. We use equations introduced by Bloch for the frequency response of magnetic moments in slowly varying external fields [3]. Hence, in the linear optics regime, we must find an expression for the permeability tensor $\boldsymbol{\mu}$ which relates the magnetization $\boldsymbol{M}$ to the external magnetic field $\boldsymbol{H}$ via $\boldsymbol{M} = \boldsymbol{\mu}(\omega)\boldsymbol{H}$.

Spectroscopic information about the response function tensor is needed to make use of the LST relation. Such spectroscopic information about magnetic resonances can be gained using terahertz Mueller matrix ellipsometry, as demonstrated recently for the N impurity in SiC [4]. Different model approaches can be employed to obtain frequencies, amplitudes, transverse relaxation times, and spin volume density parameters [4,14,15]. For example, dielectric and magnetic modes, and their hybridization in the far-infrared response of magnetodielectric $Dy_3Fe_5O_{12}$ garnet were reported by Rogers *et al.* [16]. The authors assumed isotropic response for both dielectric and magnetic resonances. Here, we present a method in which the permeability tensor derived from the Bloch equations permits one to determine the dc magnetization from the analysis of TO and LO modes associated with magnetic resonance(s). We apply this theoretical framework to experimental data obtained using our in-house built terahertz electron magnetic resonance (EPR) ellipsometer and validate our results with results from dc magnetization measurements using a superconducting quantum interference device (SQUID) magnetometer, demonstrating very good agreement. We make use of the well-known magnetic properties of Fe-doped gallium nitride (GaN) as an example.

Theory—The Bloch equations describe the time evolution of a magnetic moment vector $\boldsymbol{M}$ and can be written as [3,15,17,18]

$$\frac{\partial \boldsymbol{M}}{\partial t} = \gamma_e(\boldsymbol{M} \times \boldsymbol{H}) - \frac{\boldsymbol{M}(\hat{e}_x + \hat{e}_y)}{T_2} - \frac{(\boldsymbol{M} - \boldsymbol{M}_0)\hat{e}_z}{T_1}, \tag{5}$$

where $\times$ denotes the cross product. Here, γ_e represents the electron gyromagnetic ratio and is taken to be positive valued. The unit vectors in the laboratory coordinate system $(\hat{e}_x, \hat{e}_y, \hat{e}_z)$ correspond to the x, y, and z axes, respectively, with the z axis aligned parallel to the direction of the magnetic field. Additionally, T_1 and T_2 are the phenomenological longitudinal and transverse relaxation times, respectively. These relaxation times describe how the system returns to equilibrium when conditions, e.g., the magnetic field direction, change and contribute a wealth of information regarding the electronic structure and molecular dynamics [19]. The longitudinal relaxation time generally depends on spin-lattice interactions, and the transverse relaxation time depends on spin-spin interactions [20].

The total magnetic field is given by

$$\boldsymbol{H} = H_0\hat{e}_z + H_x(t)\hat{e}_x + H_y(t)\hat{e}_y, \tag{6}$$

where H_0 represents the static component of the magnetic field aligned with the z axis, and $H_x(t)$ and $H_y(t)$ denote the time-varying components of the magnetic field in the x and y directions, respectively. These latter components are attributed to the rotating magnetic field generated by polarized light traversing the system. Upon substituting (6) into the Bloch equations, we derive the following system of equations:

$$\begin{aligned}
\frac{\partial M_x}{\partial t} &= \omega_0 M_y - \frac{M_x}{T_2} + \gamma_e M_z H_y(t), \\
\frac{\partial M_y}{\partial t} &= -\omega_0 M_x - \frac{M_y}{T_2} - \gamma_e M_z H_x(t), \\
\frac{\partial M_z}{\partial t} &= -\frac{M_z - M_0}{T_1} + \gamma_e[M_y H_x(t) - M_x H_y(t)],
\end{aligned} \tag{7}$$

where we have introduced $\omega_0 = \gamma_e H_0$, which corresponds to the angular frequency of the magnetization's precession around the z axis. When the magnetic field components $H_x(t)$ and $H_y(t)$ are significantly smaller than H_0, a condition described as the low-power limit, the magnetization along the z axis M_z can be approximated as remaining at its equilibrium value M_0, and $\partial M_z/\partial t = 0$. This simplification implies a negligible influence of saturation effects on the system [21]. We can, in the low-power limit, further simplify by the substitution $\gamma_e M_z = \gamma_e M_0 = \gamma_e H_0 \chi_0 = \omega_0 \chi_0$, where $\chi_0 \equiv M_0/H_0$ is the dc magnetic susceptibility. By assuming that $1/T_2 \ll \omega_0$ and applying a Fourier transform, we arrive at

$$\begin{aligned}
M_x(\omega_0^2 - i\omega/T_2 - \omega^2) &= \omega_0^2 \chi_0 H_x - i\chi_0 \omega_0 \omega H_y, \\
M_y(\omega_0^2 - i\omega/T_2 - \omega^2) &= \omega_0^2 \chi_0 H_y + i\chi_0 \omega_0 \omega H_x,
\end{aligned} \tag{8}$$

where ω is the angular frequency, and in tensor form

$$\begin{pmatrix} M_x \\ M_y \end{pmatrix} = \boldsymbol{\chi_M} \begin{pmatrix} H_x \\ H_y \end{pmatrix} = \chi_0 \begin{pmatrix} \frac{\omega_0^2}{\omega_0^2 - i\omega/T_2 - \omega^2} & -i\frac{\omega\omega_0}{\omega_0^2 - i\omega/T_2 - \omega^2} \\ i\frac{\omega\omega_0}{\omega_0^2 - i\omega/T_2 - \omega^2} & \frac{\omega_0^2}{\omega_0^2 - i\omega/T_2 - \omega^2} \end{pmatrix} \begin{pmatrix} H_x \\ H_y \end{pmatrix}, \quad (9)$$

where tensor $\chi_{\mathbf{M}}$ has a structure similar to the Polder tensor for the magnetic susceptibility of ferrites [22]. To arrive at the LST relation and its generalizations, it is convenient to neglect the linewidth broadening ($1/T_2 = 0$), as it does not affect the final result. For the case of systems with spin $S > 1/2$, it is assumed that each of the $2S$ transitions adheres to the same line shape, and the Bloch permeability is written as

$$\boldsymbol{\mu} = \boldsymbol{I} + \sum_{j=1}^{2S} \begin{pmatrix} \frac{\chi_{0,j}\omega_{0,j}^2}{\omega_{0,j}^2 - \omega^2} & i\frac{\chi_{0,j}\omega\omega_{0,j}}{\omega_{0,j}^2 - \omega^2} & 0 \\ -i\frac{\chi_{0,j}\omega\omega_{0,j}}{\omega_{0,j}^2 - \omega^2} & \frac{\chi_{0,j}\omega_{0,j}^2}{\omega_{0,j}^2 - \omega^2} & 0 \\ 0 & 0 & \chi_{0,j} \end{pmatrix}, \quad (10)$$

where each of the $2S$ spin transitions contributes independently to the static susceptibility $\chi_0 = \sum_{j=1}^{2S} \chi_{0,j}$, similar to the extension of the LST relation to multiple optical phonon branches [5,6]. This analogy invites a comparison between spin and phonon transitions, given the well-characterized nature of phonon modes in low-symmetry materials [8,11]. To begin with, setting $\omega = 0$ in Eq. (10), we recover the dc response $\boldsymbol{\mu}(\omega = 0) = \mu_{\mathrm{dc}}\mathbf{I}$, where $\mu_{\mathrm{dc}} = (1 + \chi_0)$ denotes the dc magnetic permeability. It is noteworthy that this model does not capture diamagnetic contributions. Magnetic dipole transitions outside the available spectral range such as radio-frequency-induced nuclear magnetic resonance also do not contribute to the summation of χ_0. Furthermore, this derivation assumes the absence of magnetic resonances at frequencies beyond all $\omega_{0,j}$, effectively setting $\mu_\infty = 1$. We utilize the coordinate invariant LST relation and search for the eigenresonances

$$\det[\boldsymbol{\mu}^{-1}(\omega_{\mathrm{TO}})] = 0, \qquad \det[\boldsymbol{\mu}(\omega_{\mathrm{LO}})] = 0. \quad (11)$$

It can be easily verified that the determinant of $\boldsymbol{\mu}$ diverges when the frequency ω equals one of the resonant frequencies $\omega_{0,j}$. Thus, the TO modes correspond to the resonance frequencies, $\omega_{\mathrm{TO},j} = \omega_{0,j}$. However, identifying the LO modes requires a more detailed analysis. The determinant is given by [23]

$$\begin{aligned} \det(\boldsymbol{\mu}) &= \mu_{\mathrm{dc}} \left[1 + 2\sum_{j=1}^{2S} \frac{\chi_{0,j}\omega_{\mathrm{TO},j}^2}{\omega_{\mathrm{TO},j}^2 - \omega^2} + \left(\sum_{j=1}^{2S} \frac{\chi_{0,j}\omega_{\mathrm{TO},j}^2}{\omega_{\mathrm{TO},j}^2 - \omega^2} \right)^2 - \omega^2 \left(\sum_{j=1}^{2S} \frac{\chi_{0,j}\omega_{\mathrm{TO},j}}{\omega_{\mathrm{TO},j}^2 - \omega^2} \right)^2 \right] \\ &= \mu_{\mathrm{dc}} \left\{ \frac{1}{\prod_{j=1}^{2S} \omega_{\mathrm{TO},j} + \omega} P^{2S}(-\omega) \right\} \times \left[\frac{1}{\prod_{j=1}^{2S} \omega_{\mathrm{TO},j} - \omega} P^{2S}(\omega) \right]. \end{aligned} \quad (12)$$

Here, $P^{2S}(\omega)$ is a polynomial of degree $2S$, which, according to the fundamental theorem of algebra can be written as the product of its linear factors, where the roots correspond to the LO modes

$$\det(\boldsymbol{\mu}) = \mu_{\mathrm{dc}} \left\{ \prod_{j=1}^{2S} \frac{\omega_{\mathrm{LO},j} + \omega}{\omega_{\mathrm{TO},j} + \omega} \right\} \left[\prod_{j=1}^{2S} \frac{\omega_{\mathrm{LO},j} - \omega}{\omega_{\mathrm{TO},j} - \omega} \right]. \quad (13)$$

Setting $\omega = 0$ we obtain

$$\det[\boldsymbol{\mu}(\omega = 0)] = \mu_{\mathrm{dc}} \prod_{j=1}^{2S} \frac{\omega_{\mathrm{LO},j}^2}{\omega_{\mathrm{TO},j}^2} = \mu_{\mathrm{dc}}^3, \quad (14)$$

and after dividing by μ_{dc} and taking the root,

$$\mu_{\mathrm{dc}} = \prod_{j=1}^{2S} \frac{\omega_{\mathrm{LO}}}{\omega_{\mathrm{TO}}}. \quad (15)$$

Note that this is valid also for the complementary case, $\mu_{xx}(\omega) = \mu_{zz}(\omega)$, $\mu_{yy} = 1$, as the determinant will have the same form. Equation (15) is the main finding of this Letter—the magnetic analog of the LST relation. Equation (14) is independent of the choice of coordinates and thus establishes the coordinate invariant magnetic LST relation. Note the significant difference between the magnetic LST [Eq. (15)] and LST [Eq. (2)] relations, where the dielectric resonance frequencies appear squared in the latter, while the magnetic resonance frequencies appear in first order in the former. We further propose to rewrite Eq. (13) and introduce a generalized magnetic permeability function akin to the Berreman-Unterwald form [6]

$$\det[\boldsymbol{\mu}(\omega)] = \mu_{\mathrm{dc}} \prod_{j=1}^{2S} \frac{\omega_{\mathrm{LO},j}^2 - \omega^2}{\omega_{\mathrm{TO},j}^2 - \omega^2}. \quad (16)$$

Here, relaxation times $T_{2,j}$ and $T_{2,j}^\star$ can be introduced

$$\det[\boldsymbol{\mu}(\omega)] = \mu_{\mathrm{dc}} \prod_{j=1}^{2S} \frac{\omega_{\mathrm{LO},j}^2 - \omega^2 - i\omega/T_{2,j}^\star}{\omega_{\mathrm{TO},j}^2 - \omega^2 - i\omega/T_{2,j}}, \quad (17)$$

and we propose Eq. (17) to be used for analysis of measured magnetic permeability tensor spectra. Parameters $T_{2,j}, T^{\star}_{2,j}$ refer to the transverse relaxation times for resonances $\omega_{\mathrm{TO},j}$, $\omega_{\mathrm{LO},j}$, respectively. Such spectra maybe gained from investigation of polarized magnetic reststrahlen bands in ferromagnets, for example [27–29]. We demonstrate the validity of the magnetic LST relation by performing spectroscopic terahertz EPR ellipsometry measurements [4,14] and subsequent analysis using the permeability tensor in Eq. (10) including the relaxation time parameters.

We obtain the dc magnetization by summation over all transition amplitudes and compare the results with SQUID magnetization measurements. The TO modes are then known and the LO modes are then found numerically by determining the roots of Eq. (10). The product of their ratios is then tested against the results obtained from SQUID analysis as well, i.e., the validity of Eq. (15) is then confirmed.

Method—We conducted terahertz EPR ellipsometry and SQUID measurements on an iron-doped GaN sample. The sample is a bulk single crystal with c-plane (0001) surface orientation produced via halide vapor phase epitaxy, measuring approximately 8×5 mm with a thickness of 0.989 mm [23,30].

For the terahertz EPR ellipsometry measurements, we used a superconducting split-coil magnet system [31] capable of generating magnetic fields from −8 to 8 T with a field homogeneity of about 3000 ppm across the sample volume. The Mueller matrix elements were measured using a custom-built terahertz ellipsometer across a spectral range of 120–129 GHz in 50 MHz increments, employing a tunable single-frequency continuous-wave source with a frequency bandwidth of approximately 50 kHz. A solid-state synthesizer frequency source, multiplied by a signal generator extension (Virginia Diodes, Inc.), provided precise digital control over frequency and duty cycle.

Intensity readings were collected at a Golay cell detector under various polarizer and analyzer configurations to obtain the top-left 3×3 section of the Mueller matrix. Measurements were executed in a reflection setup with the sample positioned at a 45° angle of incidence between the split coils, aligning the magnetic field parallel to the incident beam. The magnetic field was oriented at 45° relative to the crystallographic c axis of the Fe-doped GaN sample. By rotating the sample around its surface normal, we aligned the two crystallographically equivalent gallium sites in the wurtzite lattice structure relative to the magnetic field. The alignment was done such that the zero-field splitting of the two different Ga site occupying Fe atoms resulted in equivalent spin levels, thereby reducing the effect of multiplicity from the quintuplet spin transitions. Thus, the two quintuplets coincide within the terahertz EPR ellipsometry spectra [15]. We selected this sample orientation for convenience, which has no effect on the results obtained in our Letter for the magnetic LST relation. We thereby reduce computation time for the data analysis procedures. One could have instead summed over all transitions when the sample has a different orientation resulting in ten individual resonances.

Measurements were conducted at a magnetic field strength of 4.42 T, repeated at −4.42 T, and also without a magnetic field to subtract background data, allowing for the extraction of small-signal difference data. The sample's temperature was maintained at 15 K throughout the measurement process. To model the response, we applied Eq. (10) (with relaxation times included) and the Berreman 4×4 matrix formalism, and we compared the model calculated data with the experimental data by minimizing the difference using a least-squares method [23].

The dc magnetic susceptibility of the Fe-doped GaN single crystal was recorded as a function of temperature under a magnetic field of 4.42 T using a SQUID magnetometer from Quantum Design, Inc. The sample was attached to a piece of paper using insulating varnish (GE Varnish, Oxford Instruments) and mounted with its plane parallel to the direction of the magnetic field. To eliminate the diamagnetic contribution, we made an additional magnetization versus magnetic field measurement. The diamagnetic susceptibility was then estimated from the slope of the high-field data and used to obtain the corrected value of the magnetization using the equation: $M_{\mathrm{corr}} = M_{\mathrm{exp}} - \chi_{\mathrm{dia}} H$, where M_{corr} is the corrected value of the magnetization, M_{exp} is the experimentally measured value, χ_{dia} is the slope of the high-field region in the magnetization versus magnetic field curve, and H is the magnetic field.

Results and discussion—The experimental results alongside the corresponding best-fit model are presented in Fig. 1. A very good agreement between the best-match model calculated and experimental data is evident. This substantiates our theoretical approach in linking optical modes with static magnetic properties, as can be done

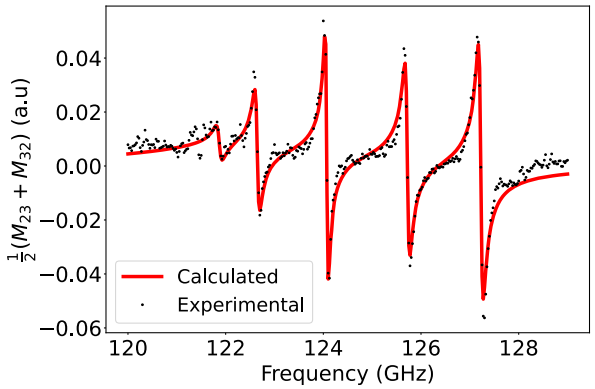

FIG. 1. Experimental (black dots) and best-match model calculated (red line) data from a frequency-swept terahertz EPR Mueller matrix measurement, performed at 15 K and magnetic field ±4.42 T. The sample is an iron-doped GaN substrate.

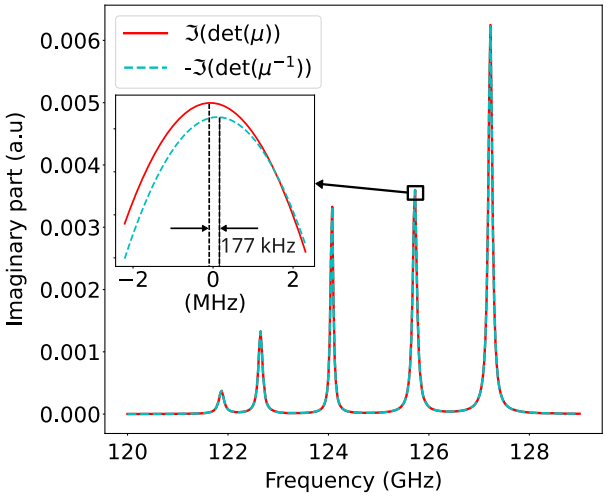

FIG. 2. Best-match-model calculated imaginary part of the determinant of the frequency-dependent permeability tensor $\boldsymbol{\mu}$ (red solid line) and the negative of the imaginary part of the determinant of the frequency-dependent inverse permeability tensor $\boldsymbol{\mu}^{-1}$ (cyan dashed line). Resonance ($\omega_{\mathrm{TO},j}$) and antiresonance ($\omega_{\mathrm{LO},j}$) peak in $\mathrm{Im}\boldsymbol{\mu}$ and $-\mathrm{Im}\boldsymbol{\mu}^{-1}$, respectively. The inset enlarges the difference between transitions $j = 4$. Note, the splitting between $\omega_{\mathrm{LO},j}$ and $\omega_{\mathrm{TO},j}$ is much smaller (few tens to few hundreds of kilohertz, see Table I) than the frequency intervals at which the data were acquired (50 MHz).

for phononic resonances that follow a Lorentzian line shape. All Mueller matrix elements are included in the Supplemental Material [23], which reveal the same good agreement for all elements. The inclusion of frequency-dependent contributions to the dielectric tensor does not improve the agreement. Hence, we can conclude that potentially existing hybridization effects between dielectric and magnetic processes are small and it can be justified to consider the resonances observed here as magnetic in nature. In Fig. 2, the imaginary parts of the calculated function $\det(\mu)$ and its inverse are plotted to illustrate the small differences between the associated TO and LO modes. For all transitions, differences are observed on the order of tens of kilohertz, and numerical values are tabulated in Table I. Measurements at kilohertz frequency intervals are needed to resolve the differences between the modes in future experiments. For the purpose of this Letter, the transitions originating at the two nonequivalent Ga sites are accounted for conveniently by rotating the sample such that the transitions are effectively pairwise equivalent, resulting in a total of five observable resonances. Hence, the sum is running over five transitions with twice the amplitude parameters. By inserting the calculated optical modes into Eq. (15), we obtain the relative static permeability of $1 + (5.4 \pm 0.2) \times 10^{-6}$ within a 95% confidence interval. We note that the largest source of uncertainty is the accuracy by which the sample thickness parameter is known [23].

TABLE I. Calculated parameters from a best-match model using nonlinear least-squares optimization on terahertz EPR ellipsometry data at 15 K and a magnetic field of ±4.42 T. Uncertainties for the last significant digit are provided in parentheses. Uncertainties for parameters $\chi_{0,j}$ and $T_{2,j}$ were estimated using the square root of the covariance matrix derived from the optimization. The uncertainties for frequencies are assumed to match uncertainty in the magnetic field strength, known to five significant digits.

j	1	2	3	4	5
$\omega_{\mathrm{TO},j}$ (GHz)	121.87(1)	122.65(1)	124.07(1)	125.72(1)	127.22(1)
$\omega_{\mathrm{LO},j}$-$\omega_{\mathrm{TO},j}$ (kHz)	23.037(1)	65.624(1)	111.12(1)	177.03(1)	301.34(1)
$\chi_{0,j}$ (10^{-8})	19(3)	54(3)	90(4)	141(5)	237(7)
$T_{2,j}$ (ns)	2.6(7)	3.2(3)	4.9(3)	3.3(2)	3.3(2)

A volume magnetization of $M_{\mathrm{Vol}} = 18.9$ A/m was obtained at 15 K from the SQUID magnetometry measurement. The static permeability is then given by the relation

$$\mu_{\mathrm{dc}} = 1 + \frac{M_{\mathrm{Vol}}}{H} = 1 + \frac{18.9\ \mathrm{A/m}}{3.52 \times 10^{6}\ \mathrm{A/m}} = 1 + 5.37 \times 10^{-6}. \quad (18)$$

Given that the SQUID measurement was conducted with the static magnetic field aligned parallel to the sample surface, i.e., with H parallel to the GaN c axis, comparison with the terahertz EPR result requires extrapolating the relative static magnetic susceptibility for a scenario where the magnetic field is oriented at 45° relative to the GaN c axis [23]. After correction of the SQUID result for the magnetic field geometry, a value of $1 + 5.32 \times 10^{-6}$ is obtained, in very good agreement with the ellipsometry result. Hence, we conclude an excellent match between the theory presented here and the results of the conducted experiments. We conclude the validity of the magnetic LST relation, therefore, for magnetic transitions such as those occurring at impurities in semiconductor materials.

In conclusion, this Letter presents the frequency dependence and tensor structure of the magnetic susceptibility for the interaction of electromagnetic waves with paramagnetic resonances, which permits correctly representing measured Mueller matrix data. Moving forward, we propose that this expression should be used to model data from polarization-resolved reflection and transmission-type optical experiments involving paramagnetic materials. A new relationship is derived and demonstrated by experiment from our tensor model which establishes the magnetic analog of the Lyddane-Sachs-Teller relationship for dipolar excitations.

Acknowledgments—This work is supported by the Swedish Research Council under Grants No. 2016-00889 and No. 2022-04812, by the Knut and Alice Wallenberg Foundation under award "Wide-bandgap semiconductors for next generation quantum components" (Grant No. 2018.0071) and "Transforming ceramics into next generation semiconductors" (Grant No. 2024.0121), by the Swedish Foundation for Strategic Research under Grant No. EM16-0024, by the Swedish Governmental Agency for Innovation Systems VINNOVA under the Competence Center Program Grant No. 2022-03139, and by the Swedish Government Strategic Research Area NanoLund and in Materials Science on Functional Materials at Linköping University, Faculty Grant SFO Mat LiU No. 009-00971. V. D. acknowledges support by the Knut and Alice Wallenberg Foundation for a Scholar award (Grant No. 2023.0349). M. S. acknowledges support by the National Science Foundation under Awards No. ECCS 2329940 and No. OIA-2044049 Emergent Quantum Materials and Technologies (EQUATE), by Air Force Office of Scientific Research under Awards No. FA9550-19-S-0003, No. FA9550-21-1-0259, and No. FA9550-23-1-0574 DEF, and by the University of Nebraska Foundation. M. S. acknowledges support from the J. A. Woollam Foundation. T. S. gratefully acknowledges funding from the Swedish Research Council (Grant No. 2021-03675).

[1] R. H. Lyddane, R. G. Sachs, and E. Teller, Phys. Rev. **59**, 673 (1941).
[2] C. F. Klingshirn, *Semiconductor Optics* (Springer, Berlin, Heidelberg, 2012).
[3] F. Bloch, Phys. Rev. **70**, 460 (1946).
[4] M. Schubert, S. Knight, S. Richter, P. Kühne, V. Stanishev, A. Ruder, M. Stokey, R. Korlacki, K. Irmscher, P. Neugebauer, and V. Darakchieva, Appl. Phys. Lett. **120**, 102101 (2022).
[5] A. S. Barker, Phys. Rev. **136**, A1290 (1964).
[6] D. W. Berreman and F. C. Unterwald, Phys. Rev. **174**, 791 (1968).
[7] W. Cochran and R. Cowley, J. Phys. Chem. Solids **23**, 447 (1962).
[8] M. Schubert, Phys. Rev. Lett. **117**, 215502 (2016).
[9] M. Schubert, A. Mock, R. Korlacki, and V. Darakchieva, Phys. Rev. B **99**, 041201(R) (2019).
[10] M. Schubert, A. Mock, R. Korlacki, S. Knight, Z. Galazka, G. Wagner, V. Wheeler, M. Tadjer, K. Goto, and V. Darakchieva, Appl. Phys. Lett. **114**, 102102 (2019).
[11] A. Mock, R. Korlacki, S. Knight, and M. Schubert, Phys. Rev. B **97**, 165203 (2018).
[12] A. Mock, R. Korlacki, S. Knight, and M. Schubert, Phys. Rev. B **95**, 165202 (2017).
[13] M. Stokey, A. Mock, R. Korlacki, S. Knight, V. Darakchieva, S. Schöche, and M. Schubert, J. Appl. Phys. **127**, 115702 (2020).
[14] S. Richter, S. Knight, O. Bulancea-Lindvall, S. Mu, P. Kühne, M. Stokey, A. Ruder, V. Rindert, V. Ivády, I. A. Abrikosov, C. G. Van de Walle, M. Schubert, and V. Darakchieva, Phys. Rev. B **109**, 214106 (2024).
[15] V. Rindert, S. Richter, P. Kühne, A. Ruder, V. Darakchieva, and M. Schubert, Phys. Rev. B **110**, 054413 (2024).
[16] P. D. Rogers, Y. J. Choi, E. C. Standard, T. D. Kang, K. H. Ahn, A. Dubroka, P. Marsik, C. Wang, C. Bernhard, S. Park, S.-W. Cheong, M. Kotelyanskii, and A. A. Sirenko, Phys. Rev. B **83**, 174407 (2011).
[17] J. A. Weil and J. R. Bolton, Relaxation times, linewidths and spin kinetic phenomena, in *Electron Paramagnetic Resonance* (John Wiley & Sons, Ltd, New York, 2006), Chap. 10, pp. 301–356.
[18] P. Baranov, I. Ilyin, and E. Mokhov, Solid State Commun. **101**, 611 (1997).
[19] S. S. Eaton and G. R. Eaton, Relaxation times of organic radicals and transition metal ions, in *Distance Measurements in Biological Systems by EPR*, edited by L. J. Berliner, G. R. Eaton, and S. S. Eaton (Springer US, Boston, MA, 2000), pp. 29–154.
[20] A. Abragam and B. Bleaney, *Electron Paramagnetic Resonance of Transition Ions* (Clarendon Press, Oxford, 1970).
[21] C. P. Slichter, Basic theory, in *Principles of Magnetic Resonance* (Springer, Berlin, Heidelberg, 1990), pp. 11–64.
[22] D. Polder, London, Edinburgh, and Dublin Philos. Mag. J. Sci. **40**, 99 (1949).
[23] See Supplemental Material at http://link.aps.org/supplemental/10.1103/PhysRevLett.134.086703 for additional information on data analysis and intermediate steps of the derivations, which includes Refs. [15,21,24–26].
[24] H. Fujiwara, Principles of optics, in *Spectroscopic Ellipsometry* (John Wiley & Sons, Ltd, New York, 2007), Chap. 2, 3, 4, pp. 13–207.
[25] S. Geschwind, Phys. Rev. **121**, 363 (1961).
[26] T. Kashiwagi, S. Sonoda, H. Yashiro, Y. Ishihara, A. Usui, Y. Akasaka, and M. Hagiwara, Jpn. J. Appl. Phys. **46**, 581 (2007).
[27] A. Lehmeyer and L. Merten, J. Magn. Magn. Mater. **50**, 32 (1985).
[28] M. R. F. Jensen, S. A. Feiven, T. J. Parker, and R. E. Camley, J. Phys. Condens. Matter **9**, 7233 (1997).
[29] W. Kullmann, K. Strobel, and R. Geick, J. Phys. C **17**, 6855 (1984).
[30] T. Paskova, R. Kroeger, S. Figge, D. Hommel, V. Darakchieva, B. Monemar, E. Preble, A. Hanser, N. M. Williams, and M. Tutor, Appl. Phys. Lett. **89**, 051914 (2006).
[31] P. Kühne, N. Armakavicius, V. Stanishev, C. M. Herzinger, M. Schubert, and V. Darakchieva, IEEE Trans. Terahertz Sci. Technol. **8**, 257 (2018).